Cent. Eur. J. Chem. • 12(4) • 2014 • 509-518
DOI: 10.2478/s11532-013-0397-y

VERSITA

Central European Journal of **Chemistry**

Interfacial behavior of water bound to nitrocellulose containing residual nitric and sulfuric acids

Research Article

Vladimir M. Gun'ko[1*], Waldemar Tomaszewski[2], Tetyana V. Krupska[3], Konstantin V. Turov[4], Roman Leboda[5], Vladimir V. Turov[3]

[1]*Department of Amorphous and Structurally Ordered Oxides, Chuiko Institute of Surface Chemistry, 03164 Kiev, Ukraine*

[2]*Department of Chemistry, Warsaw University of Technology, 00-664 Warsaw, Poland*

[3]*Department of Biomedical Problems of Surface, Chuiko Institute of Surface Chemistry, 03164 Kiev, Ukraine*

[4]*Department of Bioactive Heterocyclic Basic Compounds, Institute of Bioorganic Chemistry and Petrochemistry, 02094 Kiev, Ukraine*

[5]*Faculty of Chemistry, Maria Curie-Skłodowska University, 20-031 Lublin, Poland*

Received 4 October 2013; Accepted 19 November 2013

Abstract: To prepare nitrocellulose (NC), microcrystalline cellulose was treated in a mixture of nitric and sulfuric acids. Prepared NC containing a small amount of acids was studied at a different hydration degree (h = 10-1000 mg g^{-1}) in different dispersion media (chloroform-d, acetone-d_6 or their mixtures) using low-temperature ^{1}H NMR spectroscopy. The hydration degree and the presence of residual acids affected the temperature dependence of the chemical shifts of proton resonance of water bound to NC. The Gibbs free energy of bound water became less negative with increasing hydration rate. The chloroform and acetone media affect the behavior of bound-to-NC water unfrozen at T<273 K differently. Quantum chemical calculations were performed using *ab initio* (HF/6-31G(d,p)), DFT (B3LYP/6-31G(d,p)) and semiempirical PM7 methods to analyze the interfacial behavior of water interacting with NC containing residual amounts of nitric and sulfuric acids.

Keywords: *Nitrocellulose • Adsorbed water • Co-adsorbed organic solvents • Residual nitric and sulfuric acids • Low-temperature ^{1}H NMR spectroscopy*

1. Introduction

The application of nitrocellulose (NC), especially as a propellant [1], has a long history. NC plasticized by acetone or ethers was used in transparent photosensitive materials (celluloids, collodion) [2]. NC was applied to prepare nitropaints and decorative coats in paint and varnish industry [3].

Nitrocellulose has fiber-like or lamellar structures, a yellowish white color, and is similar to initial cellulose (cotton); however, many of the properties of NC and pure cellulose strongly differ. One of the main characteristics of NC is the degree of substitution of cellulose hydroxyls by nitro groups. The complete substitution gives trinitrate cellulose (explosive pyroxylin, guncotton) (Fig. 1a).

The physical properties of NC (as well as initial cellulose), including its explosive characteristics, depend strongly on the content of adsorbed water. Like cellulose, NC is insoluble in water. However, it can adsorb a significant amount of water due to significant polarity of

* *E-mail: vlad_gunko@ukr.net*

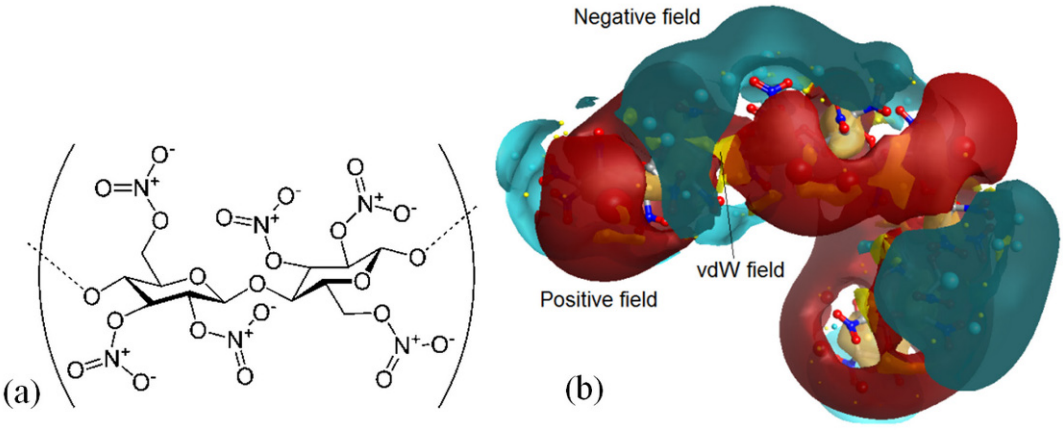

Figure 1. (a) Scheme of nitrocellulose, and (b) fields around a NC chain (calculated using TorchLite 10.0.1 [4,5]).

the rings (Fig. 1b) with side nitro groups and oxygen atoms in the side groups and the rings. Notice that at a high hydration degree h > 0.5 g of water per gram of dry material, NC loses its explosive properties [6-8].

High-polar NC chains bind a great amount of water [9], thus affecting the water structure, which also depends on the hydration degree of NC and the presence of co-adsorbates. Bound water structure can be studied in detail using low-temperature ^{1}H NMR spectroscopy with step-by-step freezing-out of bulk and interfacial water layers [10,11]. This approach allows one to estimate not only the temperature dependence of the amounts of unfrozen bound water, but also changes in the Gibbs free energy of this water depending on its content and temperature and the size distribution of pores filled by water unfrozen at T < 273 K. The interfacial behavior of water can change in the presence of nonpolar or polar co-adsorbates or solutes [11] that allow one to control the properties of wetted materials. The characteristics of adsorbed water are especially sensitive to the presence of such ion-generating solutes as strong acids [12-15].

Interfacial water can be divided into weakly (WAW) and strongly (SAW) associated waters characterized by low (δ_H =1-2 ppm) and high (δ_H > 3 ppm, ~7 ppm for ice Ih) values of the chemical shift of the proton resonance (δ_H), respectively [11]. WAW corresponds to 1D or strongly branched 2D or 3D structures. SAW has a more compacted 3D structure (spherical drops are within the limit) with a greater average number of the hydrogen bonds per molecule than WAW. The SAW/WAW ratio depends on water content, adsorbent porosity and surface structure, as well as on the type and content of co-adsorbates and dispersion media.

Strong acids are characterized by great δ_H values up to 13 ppm due to the significant diminution of electron density on acidic H atoms [9]. The δ_H values depend on the water content in the acidic solutions or on the content of water and acid co-adsorbed onto an adsorbent surface [11-15]. Fast proton exchange between hydroxyls of acids and water in the aqueous solutions of acids leads to an increase in the δ_H values of water. Confined space effects, which increase with decreasing pore sizes, can lead to a decrease in the activity of water as a solvent. This results in the differentiation of the aqueous solutions of acids by the δ_H values for the mixtures located in pores of different sizes [11-15]. Confined space effects can be observed in porous or swollen polymers or hydrogels [11,16]. One can assume that similar effects can occur in nitrocellulose which are differently hydrated and in different dispersion media.

This purpose of studied structural features and temperature dependence of the behavior of water bound to nitrocellulose and which contained residual amounts of nitric and sulfuric acids used on the NC synthesis in different dispersion media (chloroform-d, acetone-d_6 and $CDCl_3$/$(CD_3)_2CO$ mixtures). Note that acetone was used as an agent plasticizing NC.

2. Experimental procedure

2.1. Materials

Microcrystalline cellulose, MCC (Fluka) (Figs. 2a, 2b) was used as the initial material to prepare nitrocellulose (Figs. 2c, 2d) using a method described in detail elsewhere [1,2,7,8].

MCC nitration was carried out using a mixture of nitric (anhydrous, 100%) and sulfuric (98%) acids (70 mL). MCC (10 g) was added in small amounts to the acid mixture at 25°C. Then the mixture was stirred at 25°C for 18 h. The reaction mixture was added to ice water (200 mL). The NC residue was filtrated and washed by cool water (50 mL), and then dried at 25°C for three days. The nitration degree of the cellulose

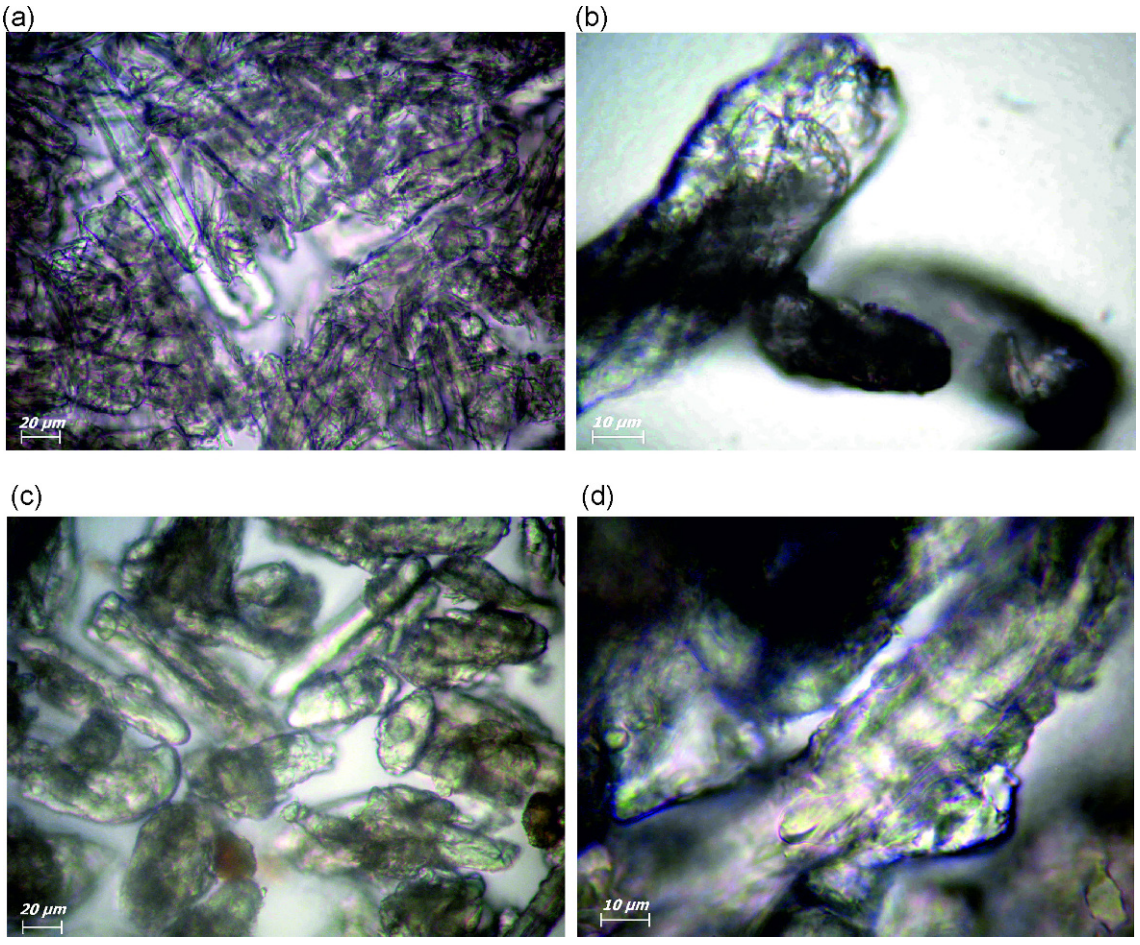

Figure 2. Microphotographs (Primo Star optical microscope, Carl Zeiss) of (a, b) hydrated MCC and (c, d) NC with magnification: (a, c) ×400 and (b, d) ×1000 (scale bar 20 μm (a, c) and 10 μm (b, d)).

was approximately 100% as the nitrogen content was ~14 wt.% determined by the Dumas method [17]. NC contained small residual amounts of acids (~2 wt.%) which affected the behavior of water bound to NC. NMR measurements were performed for 4 days after NC synthesis to avoid NC degradation under acid action.

Deuterated chloroform $CDCl_3$ and acetone $(CD_3)_2CO$ (grade for NMR spectroscopy) were used as solvents which did not effectively contribute to the ^1H NMR spectra of water bound to NC. These solvents had small amounts of non-deuterated admixtures $CHCl_3$ and $(CH_3)_2CO$ characterized by δ_H = 7.2 and 2.2 ppm, respectively, in respect to tetramethylsilane (TMS) at δ_H = 0 ppm.

2.2. ^1H NMR spectroscopy

The ^1H NMR spectra were recorded at 210-280 K using a Varian 400 Mercury spectrometer (magnetic field of 9.4 T) of high resolution with the probing 90° pulses at a duration of 3 μs with eight scans and a 2 s delay, as well at a bandwidth of 20 kHz. Relative mean errors were smaller than ±10% for ^1H NMR signal intensity for the overlapped signals and ±5% for the single signals, and ±1 K for the temperature. To prevent supercooling of the systems, the temperature dependences of concentration of unfrozen adsorbates were determined during the heating of the samples that were pre-cooled to 210 K. The signals of protons from water molecules in ice and from H atoms in NC did not contribute to the recorded ^1H NMR spectra because of the measurement techniques that were applied to the static samples [10,11] and the short time of the transverse relaxation of protons in solids or immobile polymers.

Specific amounts of distilled water and a solvent ($CDCl_3$, $(CD_3)_2CO$ or their mixture) were added to air-dry nitrocellulose (initial hydration degree h = 10 mg g^{-1}) to prepare hydrated samples. Before measurements were taken, samples (placed in closed NMR ampoules) were shaken for 10 min and then equilibrated for 1 h (the samples were uniform in the sensor gap because the spectra were identical with and without a sample rotation). To determine the chemical shift of the proton

resonance, δ_H, tetramethylsilane (TMS) was used as an internal standard (δ_H = 0 ppm) added to $CDCl_3$ in the amount of 0.2 wt.%.

The amount of unfrozen NC-bound water (C_{uw}) as a function of temperature at T < 273 K was estimated by comparing the integral intensity (I_{uw}) of total ^{1}H NMR signal of unfrozen water to that of total water at T > 273 K using a calibrated function $I_C = f(C_{H2O})$, assuming $C_{uw} = C_{H2O}\, I_{uw}/f(C_{H2O})$ [10,11].

Changes in the Gibbs free energy of ice with temperature [18] were calculated as follows:

$$\Delta G_{ice} = 0.0295 - 0.0413\Delta T + 6.64369\times10^{-5}(\Delta T)^2 + \\ +2.27708\times10^{-8}(\Delta T)^3 \text{ (kJ mol}^{-1}\text{)}, \quad (1)$$

where $\Delta T = 273.16 - T$ at $T \le 273.15$ K. Eq. 1 was used to estimate the $\Delta G(T)$ function for water bound to NC [10,11]. The $C_{uw}(T)$ and $\Delta G(T)$ functions can be easily transformed into the relationship between C_{uw} and ΔG.

Water can be frozen in narrower pores at lower temperatures as described by the Gibbs-Thomson relation for the freezing point depression for liquids confined in cylindrical pores at radius R [19-22]

$$\Delta T_m = T_{m,\infty} - T_m(R) = -\frac{2\sigma_{sl}T_{m,\infty}}{\Delta H_f \rho R} = \frac{k}{R}, \quad (2)$$

where $T_m(R)$ is the melting temperature of ice in cylindrical pores of radius R, $T_{m,\infty}$ the bulk melting temperature, ΔH_f the bulk enthalpy of fusion, ρ the density of the solid, σ_{sl} the energy of solid-liquid interaction, and k is a constant. Eq. 2 was used to determine the distribution function ($f_V(R) = dV_{uw}(R)/dR$) of sizes of water structures unfrozen at T < 273 K [19-22] adsorbed onto nitrocellulose using equation [11]:

$$\frac{dV_{uw}(R)}{dR} = \frac{A}{k}(T_m(R) - T_{m,\infty})^2 \frac{dC_{uw}(T)}{dT}, \quad (3)$$

where $V_{uw}(R)$ is the volume of unfrozen water in pores of radius R, C_{uw} is the amount of unfrozen water per gram of nitrocellulose as a function of temperature, and A is a constant. The $f_V(R)$ function can be used to determine the distribution function in respect to the specific surface area of the NC structures contacting with unfrozen water [11]

$$f_S(R) = \frac{w}{R}\left(\frac{dV_{uw}(R)}{dR} - \frac{V_{uw}(R)}{R}\right) \quad (4)$$

where w is the form-factor equal to 2 for cylindrical pores. Integration of the $f_S(R)$ function gives the specific surface area (S_{uw}) of the contact area between unfrozen water and a surface of nitrocellulose particles [11]. Note that the application of the NMR cryoporometry to a variety of solid and soft materials gave reliable structural characteristics compared with those based on the data of the standard adsorption methods [10-16,19-22].

The average freezing temperature <T> was calculated using expression [11]

$$< T >= \int_{T_{min}}^{T_0} T(dC_{uw}(T)/dT)dT \Big/ \int_{T_{min}}^{T_0} (dC_{uw}(T)/dT)dT, \quad (5)$$

where T_0 = 273.15 K, and T_{min} is the temperature corresponding to C_{uw} = 0.

3. Computation details

The geometry optimization of molecular clusters was carried out using HF/6-31G(d,p) with the Gaussian 09 [23] or Firefly 8.0 [24] packages. The NMR spectra of these clusters were calculated using the gauge-independent atomic orbital (GIAO) method and taking the solvation effects using the SMD [25] method with B3LYP/6-31G(d,p) into consideration [23]. The δ_H values were calculated as the difference between the isotropic values (average value of diagonal values of the magnetic shielding tensor of protons, $\sigma_{H,iso}$) of TMS ($\sigma_{H,iso}$ = 31.76 ppm using GIAO/B3LYP/6-31G(d,p)) and the studied compounds $\delta_H = \frac{1}{3}Tr\sigma_{TMS} - \frac{1}{3}Tr\sigma_H$.

Large systems (up to 2000-3000 atoms) were studied using the semiempirical PM7 method (MOPAC 2012) [26]. The δ_H values were calculated using a correlation function $\delta_H = -27.97889 + 87.56668q_H$ (where q_H is the Mulliken charge of the H atoms calculated using the PM7 method). This function was obtained using the B3LYP/6-31G(d,p) (δ_H) and PM7 (q_H) results for the same systems [27]. The distribution functions of the δ_H values were calculated using the following simple expression [27]

$$f(\delta_H) = (2\pi\sigma^2)^{-0.5}\sum_j \exp[-(\delta_j - \delta_H)^2/2\sigma^2] \quad (6)$$

where j is the number of H atoms in the system, σ^2 is the distribution dispersion, and δ_j is the calculated value of the chemical shift of the j-th H atom.

4. Results and discussion

^{1}H NMR signals of water bound to NC depend strongly on the amounts of water and co-adsorbates (solvents) (Figs. 3 and 4). Air-dry NC shows that the amount of adsorbed water is low (h = 10 mg g^{-1}). The sample placed into the $CDCl_3$ medium is characterized by a broad signal in the 8-12 ppm range (Fig. 3a). The significant downfield shift of the water signal is due to the presence of residual acids (~2 wt.%) adsorbed

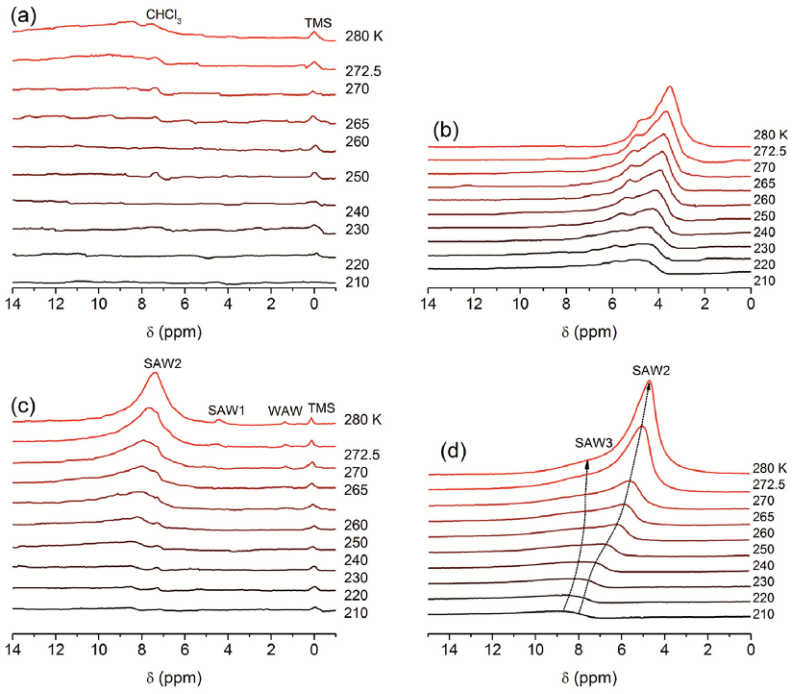

Figure 3. ^{1}H NMR spectra of water bound to NC ($CDCl_3$ medium) at different hydration h = (a, b) 10 mg g^{-1}, (c) 60 mg g^{-1} and (d) 1 g g^{-1}; (b) after addition of NaOH to neutralize residual acids.

onto NC, since bulk water (SAW) gives a signal at 4.5-5.5 ppm [11]. Signals at 0 and 7.2 ppm (Fig. 3a) corresponds to tetramethylsilane (TMS), added as a standard into chloroform, and the H atoms in $CHCl_3$ as an admixture in $CDCl_3$, respectively.

The addition of solid NaOH (10 wt.%) to the air-dry NC sample stirred results in the upfield shift of the signal close to that of bulk water (Fig. 3b) due to the neutralization of the residual acids. The calculation of the sizes of water structures bound to the initial NC showed that despite a low content of water, it formed relatively large SAW structures (Fig. 5b). This water was weakly bound water (WBW) which was frozen at T < 265 K at ΔG > −0.5 kJ mol^{-1} (Fig. 5a). The formation of relatively large water structures at small water content was due to the influence of weakly polar chloroform medium on adsorbed water that led to the diminution of the boundary area between immiscible chloroform and water (if the latter formed structures as large as possible [11]).

After adding 50 mg g^{-1} of distilled water to the initial NC sample (resulting in the total hydration degree h = 60 mg g^{-1}) and placingit into the chloroform medium, the signal intensity increases at 7-9 ppm (Fig. 3c). The chemical shift of the main signal (SAW2) changed from 7.3 ppm at 280 K to 9 ppm at 210 K. Besides this signal, two signals were observed at 1.5 ppm (WAW) and 4.5-5.0 ppm (SAW1). The latter was observed at T > 260 K, *i.e.*, this was WBW. The δ_H values of the last two signals suggested that bound water did not dissolve residual acids, which were mixed only with SAW2 characterized by a certain downfield shift.

At a higher hydration degree (h = 1 g g^{-1}) of NC, signal SAW2 has a shoulder SAW3 at greater δ_H values (Fig. 3d); *i.e.*, this water corresponds to a more concentrated solution of acids than water responsible of signal SAW2. The main changes in SAW signal intensity link with SAW2. The concentration of acids in an unfrozen solution with decreasing temperature has caused a greater shift of the SAW2 signal than that of SAW3 signal. This has resulted in the merging of SAW3 and SAW2 signals at T < 240 K.

Adding a small amount of acetone and acetone plasticizing NC into the chloroform medium, results in significant changes in the ^{1}H NMR spectra of water bound to NC (Fig. 4a). Signals of SAW2 and SAW3 are observed over the total temperature range. SAW3 is characterized by great downfield shifts up to δ_H = 13 ppm at 210 K. At T < 240 K, signal at very high δ_H = 19 ppm is observed that is characteristic for the strong symmetric hydrogen bonds [26] for solvated protons [29]. The signal at 2.2 ppm is due to the CH_3 groups in non-deuterated acetone as an admixture in $(CD_3)_2CO$.

Acetone, which is a plasticizer of NC and miscible with water, affects the 3D structure of swollen nitrocellulose particles. These effects are well seen upon comparison

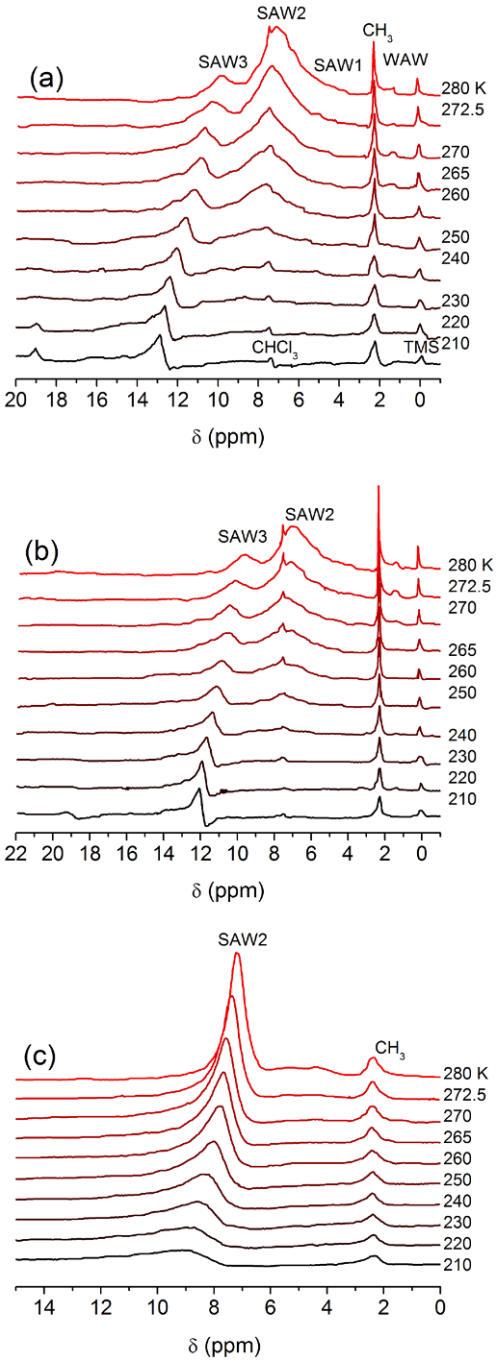

Figure 4. ^{1}H NMR spectra of water bound to NC in different media with $CDCl_3/(CD_3)_2CO$ mixtures at the ratio: (a) 15/1 and (b) 5/2 and in acetone at h = (a, b) 38 mg g^{-1} and (c) 100 mg g^{-1}.

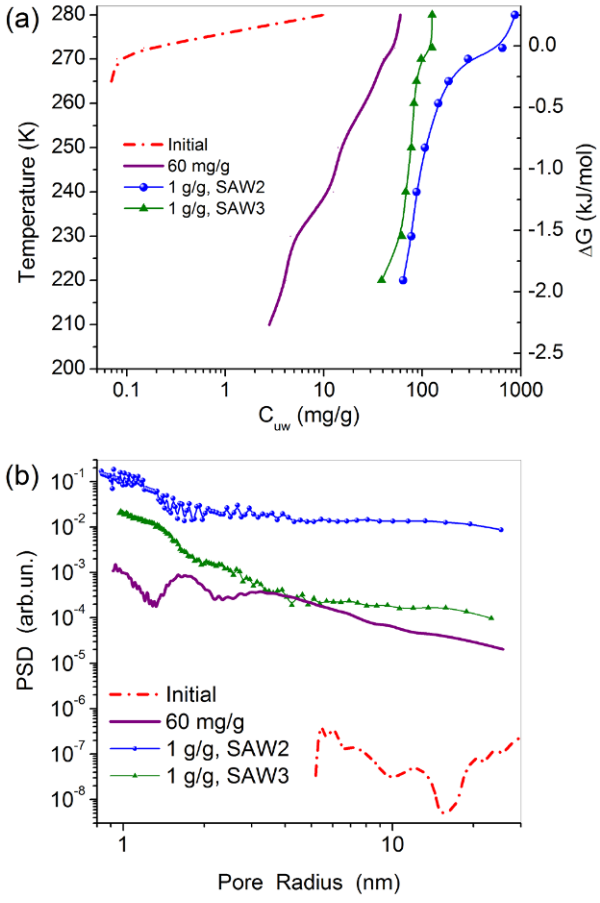

Figure 5. (a) Temperature dependences of the amounts of unfrozen water $C_{uw}(T)$ and the relationship between C_{uw} and ΔG for water bound to NC in chloroform-d medium at h = 10 (initial NC), 60 and 1000 mg g^{-1}; at h = 1000 mg g^{-1}, curves for SAW2 and SAW3 are shown. (b) Size distribution of water structures or sizes of pores in NC filled by unfrozen water.

of the textural characteristics of NC at h = 1 g g^{-1} without acetone (in the $CDCl_3$ medium) and at h = 0.1 g g^{-1} in the acetone-d_6 medium and in the $CDCl_3/(CD_3)_2CO$ mixtures (Table 1). The rearrangement of the NC structure under the acetone affects changes in the structure of the water clusters bound to the NC particles (Figs. 5 and 6). An increase in the acetone content in the $CDCl_3/(CD_3)_2CO$ mixture at their ratio 5/2 weakly affects the spectra (Figs. 4a and 4b), and the NC particles remain powdered. However, in the pure acetone medium, the signal at 19 ppm is absent (Fig. 4c), and the swollen NC looks as a non-powdered material. The splitting of signals of SAW2 and SAW3 has vanished and the signal of SAW2 at 7.2-9 ppm has become more intensive especially at low temperatures. Additionally, SAW1 signal at 4-5.5 ppm (corresponding to weakly bound water since it disappeared at T < 260 K) has two components but without them clearly splitting. SAW1 does not dissolve the acids because their signal (4-5.5 ppm) corresponds to bulk water.

Changes in the water content and the dispersion media affect the temperature behavior of bound water shown here as the amounts of unfrozen water as a function of temperature ($C_{uw}(T)$) and the relationships

Table 1. Characteristics of unfrozen water bound to nitrocellulose in different media and at different hydration degree.

Medium	h (mg g^{-1})	C_{uw}^{s} (mg g^{-1})	C_{uw}^{w} (mg g^{-1})	$-\Delta G_s$ (kJ mol^{-1})	γ_S (J g^{-1})	γ_S' (mJ m^{-2})	$<T>$ (K)	S_{uw} (m^2 g^{-1})	S_{nano} (m^2 g^{-1})	S_{meso} (m^2 g^{-1})	V_{nano} (cm^3 g^{-1})	V_{meso} (cm^3 g^{-1})	V_{macro} (cm^3 g^{-1})
$CDCl_3$	10	0	1	0.5	0	0	271.1	0.03	0	0.01	0	0	0.001
$CDCl_3$	60	26.5	33.5	2.63	2.1	300	250.9	7	3	4	0.001	0.043	0.014
$CDCl_3$	1000	203	797	3.00	24.4	195	255.4	125	82	43	0.038	0.467	0.495
$CDCl_3/(CD_3)_2CO$ (15/1)	38	26.0	12.0	2.31	2.3	767	239.7	3	0	3	0	0.033	0.005
$CDCl_3/(CD_3)_2CO$ (5/2)	38	14.5	23.5	2.31	1.1	440	255.0	2.5	0	2.4	0	0.029	0.009
$(CD_3)_2CO$	100	63	37	2.90	8.1	105	224.2	77	71	6	0.032	0.048	0.020

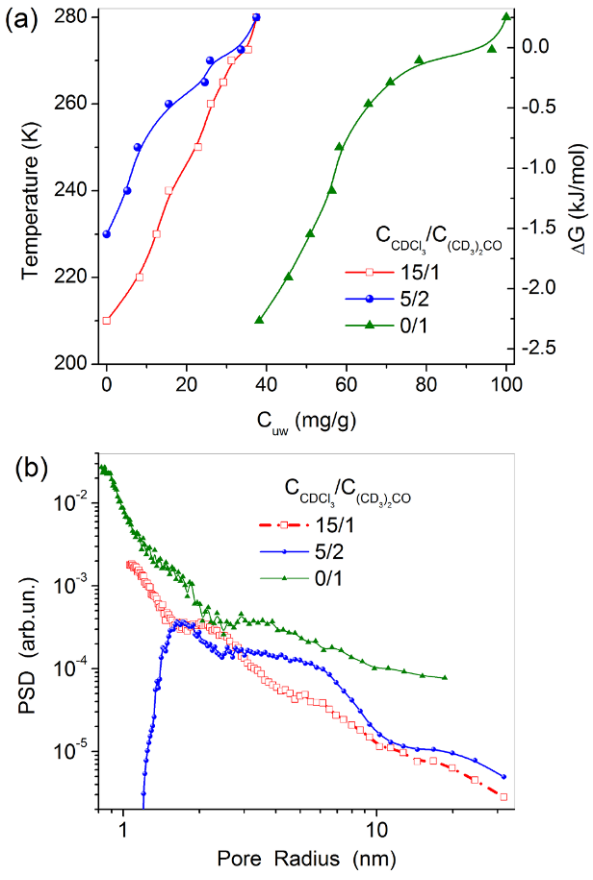

Figure 6. (a) Temperature dependences of the amounts of unfrozen water $C_{uw}(T)$ and the relationship between C_{uw} and ΔG for water bound to NC in chloroform-d/acetone-d_6 medium (their ratio is 15/1 and 5/2) at h = 38 mg g^{-1}, and in acetone-d_6 at h=100 mg g^{-1}. (b) Size distribution of water structures or sizes of pores in NC filled by unfrozen water.

between C_{uw} and changes in the Gibbs free energy of bound water (Figs. 5a and 6a).

In the initial NC placed in the chloroform-d medium, all water is weakly bound [11] since it is completely frozen at T < 260 K and the changes in the Gibbs free energy are due to its interaction with NC small as ΔG > −0.5 kJ mol^{-1} (Fig. 5a). An increase in the water content to 60 mg g^{-1} leads to changes in the temperature behavior of water and almost half of the amount (26.5 mg g^{-1} from 60 mg g^{-1}) corresponds to strongly bound water (SBW) (Table 1, C_{uw}^{s}). At h =1 g g^{-1}, a fraction of SBW corresponds to approximately 20%. This diminution of the SBW content is due to a relatively small surface area of NC being in contact with unfrozen water (Table 1, S_{uw}) at a relatively small volume of water located in narrow "pores" of NC at R < 1 nm (Table 1, V_{nano}) at much greater amounts of unfrozen water filled mesopores (V_{meso}) at 1 nm < R < 25 nm and macropores (V_{macro}) at R > 25 nm. However, nanopores (Table 1, S_{nano}) contribute most to S_{uw}.

At h = 1 g g^{-1}, the γ_S' value (Table 1) is greater than the modulus of changes in the Gibbs free energy of water interaction with NC $|\Delta G_{SL}|$ = 127.6 mJ m^{-2} estimated from the contact angle (θ) of water drops located on the NC surface and the surface tension of water (γ_L) using the Young-Dupré equation $\Delta G_{SL} = -\gamma_L(1+\cos\theta)$ at γ_L = 72.8 mJ m^{-2} and θ = 45.68° [30]. The γ_S' value calculated here can be enhanced due to the presence of residual acids bound to NC. The acid effect on the γ_S' value increases with decreasing content of water (Table 1). Additionally, the chloroform or acetone medium, *i.e.*, co-adsobates for water, can affect the changes in the Gibbs free energy. For example, in the pure acetone medium (*i.e.*, without chloroform), the γ_S' value is minimal (Table 1) and it is smaller than $|\Delta G_{SL}|$. Additionally, an increase in the acetone content in the mixture with chloroform leads to a decrease in the γ_S' value. An increase in the content of water bound to NC in the chloroform medium is accompanied by a decrease in the γ_S' value. The mention diminution in the γ_S' value corresponds to an increase in the content of unfrozen water located in narrow pores at R < 1 nm (Table 1, S_{nano}, V_{nano}). This effect with respect the γ_S' value can be explained by the diminution of the water activity as a solvent with enhancement of the confined space effects, *i.e.*, water in narrower pores can more poorly dissolve acids than water located in broader pores. Contrary, the

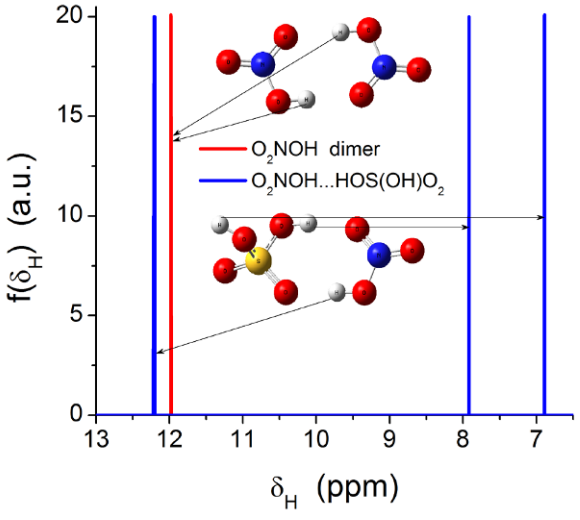

Figure 7. Calculated ^{1}H NMR spectra (GIAO/SMD/B3LYP/6-31G(d,p), water as a solvent) of dimers nitric acid and dimer with nitric and sulfuric acids.

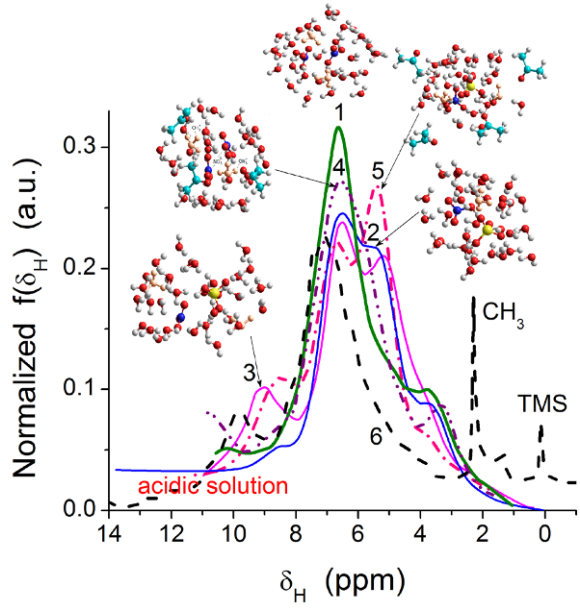

Figure 8. Calculated ^{1}H NMR spectra (PM7 with the calibration function) of (1) dimer of nitric acid with dissolution of NO-H bonds and transfer of two protons toward water molecules; dimer of nitric and sulfuric acids with dissolution of (2) NO-H and (3) NO-H and one SO-H; (4) complex (1) with addition three acetone molecules; (5) complex (3) with addition of four acetone molecules; (6) experimental ^{1}H NMR spectrum (Fig. 4a, T = 280 K).

greater the content of dissolved acids, the higher the γ_s' value is. However, the enhancement of the nanoporosity of NC causes an increase in the $-\Delta G_s$ and C_{uw}^{s} values (Table 1) characterizing the strongly bound water. This is due to the enhancement of the confined space effects in nanopores as it is described by the Gibbs-Thomson Eq. 2.

The average freezing temperature <T> (Table 1) depends on the amount and structure of water and the PSD of the adsorbent. If a fraction of bulk water or water located in macropores increases (*i.e.*, the C_{uw}^{w}/C_{uw} ratio and the V_{macro} value increase) then the <T> value increases. If the contribution of water located in nanopores increases then the <T> value decreases. Additionally, if co-adsorbate (or a liquid dispersion medium) displaces water from narrower pores into broader pores then the <T> value increases. The maximal <T> value is observed for the initial NC with minimal water content (10 mg g^{-1}) placed into the chloroform medium. This is due to the displacement of water from the NC surface by chloroform.

The GIAO/SMD/B3LYP/6-31G(d,p) calculations with consideration of the solvation effects in the aqueous medium show (Fig. 7) that the strongest downfield shift is characteristic for the protons in the bonds NO−H···O=S in the sulfuric-nitric acid dimer. A similar shift is for protons in the symmetric dimer of nitric acids. If the dimers of acids are in the water cluster (modeling a diluted solution) then the chemical shift can be smaller (comp. Figs. 7 and 8).

The addition of acetone to the cluster changes the intensity of the peaks and slightly affects their position. The maximal shifts (δ_H = 12-14 ppm) are observed for the hydrated dimer of nitric and sulfuric acids (Fig. 8, curve 2). For the hydrated dimer of nitric acid with the presence of acetone, the maximal δ_H value is equal to 11 ppm (Fig. 8, curve 4) and without acetone it is 10.5 ppm (curve 1). As a whole, the δ_H values for acidic structures are in the 8-14 ppm range. Water gives two-three peaks around 6.5 ppm (water molecules located close to acidic protons), 5 ppm (strong hydrogen bonds of the water-water type) and 3-3.5 ppm (weaker hydrogen bonds). The protons which do not participate in the hydrogen bonds are characterized by small shifts δ_H < 2 ppm.

Water molecules bound to NC are characterized by the δ_H values from 9 to 0 ppm with two main maxima at 5.5 ppm (water-water interactions) and 3 ppm (water-NC interactions, Fig. 9, curve 1). The addition of the chloroform molecules weakly affects the ^{1}H NMR spectrum (curve 2) because water forms relatively large clusters non-bound or bound to NC. However, the intensity of a peak at 3 ppm related to water molecules bound to NC, decreases. Thus, chloroform can displace a fraction of the water from the NC surface. This corresponds to the experimental data (discussed above) on the influence of chloroform on the structure of bound water. The addition of molecules of acetone, nitric and sulfuric acids to this system causes the downfield shift of the spectrum (curve 3) and appearance of a small

peak (since only four nitric and four sulfuric molecules were added) at 12 ppm. The peak of water bound to NC observed at 3 ppm decreased, as well as a shoulder observed at 5 ppm.

5. Conclusion

Residual nitric and sulfuric acids (~2 wt.%) adsorbed onto nitrocellulose affected the temperature behavior of water bound to NC, which formed different structures possessing a different ability to dissolve these acids. The acids were dissolved only in strongly associated water, which were characterized by ^{1}H NMR signals with significant downfield shifts at δ_H = 7.2-13 ppm. This water formed relatively large clusters and domains. Weakly associated water (δ_H = 1-2 ppm) did not dissolve acids. At a greater content (hydration degree 1 g g^{-1}) of water bound to NC placed in chloroform-d, there are two types of strongly associated water, which can dissolve different amounts of acids and were characterized by different downfield shifts of 7-8 and 10-13 ppm. These two forms of strongly associated water differently dissolved nitric and sulfuric acids. These water structures could be under different confined space effects. The stronger the confined space effects, the lower the water activity acted as a solvent and the smaller amount of acids could be dissolved in this water. Acetone plasticizing NC changed the confined space effects for water bound to NC. Therefore, the water activity changed with respect to adsorbed acids. In the acetone/chloroform mixtures, the behavior of water bound to NC differed compared to the individual dispersion media.

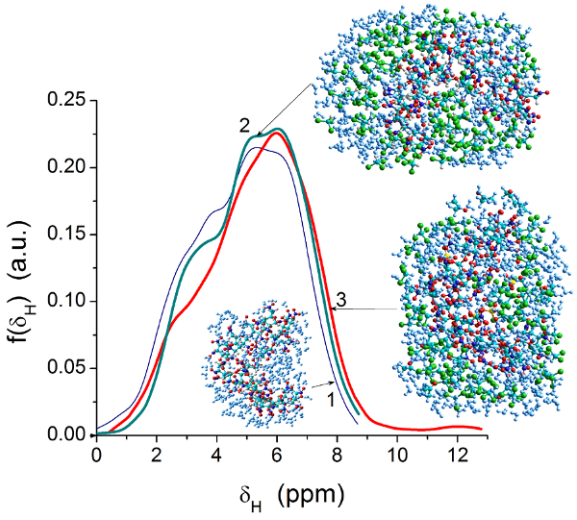

Figure 9. Calculated ^{1}H NMR spectra (PM7 with the calibration function) of water molecules (177H_2O (curve 1), 364H_2O (2) or 281H_2O (3)) bound to two NC fragments with 400 atoms (1) without and with co-adsorbed molecules of (2) chloroform (50 molecules) and (3) chloroform (50 molecules), acetone (20 molecules), nitric (four molecules) and sulfuric (four molecules) acids.

Theoretical calculations showed that even small amounts of sulfuric and nitric acids could provide the downfield shifts of the water signal, and a signal of strongly acidic protons was visible at 12 ppm.

References

[1] E.Yu. Orlova, Chemistry of High Explosives (Chemistry, Leningrad, 1973) (in Russian)

[2] P.C. Painter, M.M. Coleman, Essentials of Polymer Science and Engineering (DEStech Publications, Inc., Lancaster, USA, 2009)

[3] R. Talbert, Paint Technology Handbook (Grand Rapids, Michigan, USA, 2007)

[4] T. Cheeseright, M. Mackey, S. Rose, J.G. Vinter, Expert Opin. Drug Discov. 2, 131 (2007)

[5] TorchLite 10.0.1 www http://www.cresset-group.com/products/torch/torchlite/ (accessed Sept 4, 2013)

[6] A. Beveridge (Ed.), Forensic Investigations of Explosions (Taylor & Francis, London, 2003)

[7] T. Urbanski, Chemistry and Technology of Explosives (Pergamon Press, New York, 1964) vol. 2

[8] V.I. Gindich, L.V. Zabelin, G.N. Marchenko, Production of Cellulose Nitrates. Technology and Equipment (Central Research Institute of Scientific and Technical Information, Moscow, 1984) (in Russian)

[9] J.A. Pople, W.G. Schneider, H.J. Bernstein, High-Resolution Nuclear Magnetic Resonance (McGraw-Hill Book Company, New York 1959)

[10] V.M. Gun'ko et al., Adv. Colloid Interface Sci. 118, 125 (2005)

[11] V.M. Gun'ko, V.V. Turov, Nuclear Magnetic Resonance Studies of Interfacial Phenomena (CRC Press, Boca Raton, 2013)

[12] V.V. Turov et al., Colloids Surf. A: Physicochem. Eng. Aspects 390, 48 (2011)

[13] V.M. Gun'ko et al., J. Colloid Interface Sci. 368, 263 (2012)

[14] V.M. Gun'ko et al., Carbon 57, 191 (2013)

[15] V.M. Gun'ko et al., Adsorption 19, 305 (2013)

[16] Yu.E. Shapiro, Prog. Polymer Sci. 36, 1184 (2011)

[17] G.K. Buckee, J. Inst. Brew. 100, 57 (1994)

[18] V.P. Glushko (Ed.), Handbook of Thermodynamic Properties of Individual Substances (Nauka,

Moscow, 1978) (in Russian)
[19] D.P. Gallegos, K. Munn, D.M. Smith, D.L. Stermer, J. Colloid Interface Sci. 119, 127 (1986)
[20] J.H. Strange, M. Rahman, E.G. Smith, Phys. Rev. Lett. 71, 3589 (1993)
[21] J. Mitchell, J.B.W. Webber, J.H. Strange, Physics Reports 461, 1 (2008)
[22] O.V. Petrov, I. Furó, Prog. Nuclear Magn. Reson. Spectr. 54, 97 (2009)
[23] M. J. Frisch et al, Gaussian 09, Revision D.01 (Gaussian, Inc., Wallingford CT, 2013)
[24] A. A. Granovsky, J. Chem. Phys. 134, 214113 (2011)
[25] A.V. Marenich, C.J. Cramer, D.G. Truhlar, J. Phys. Chem. B 113, 6378 (2009)
[26] J.J.P. Stewart, MOPAC 2012, Versions 13.234W and 13.234L (Stewart Computational Chemistry, Colorado Springs, CO, USA, 2013) http://openmopac.net/
[27] V.M. Gun'ko, J. Theor. Comput. Chem. 2, 1 (2013)
[28] I.P. Gragerov, V.K. Pogorelyi, I.F. Franchuk, The Hydrogen Bond and Fast Proton Exchange (Naukova Dumka, Kiev, 1978) (in Russian)
[29] R.P. Bell, Proton in Chemistry (Chapman and Holly, London, 1959)
[30] D. Grasso, J.C. Carrington, P. Chheda, B. Kim, Water Res. 29, 49 (1995)